MOLECULAR ENDOCRINOLOGY

# Glucagon Deficiency Reduces Hepatic Glucose Production and Improves Glucose Tolerance In Adult Mice

Aidan S. Hancock, Aiping Du, Jingxuan Liu, Mayumi Miller and Catherine L. May

Mol. Endocrinol. 2010 24:1605-1614 originally published online Jun 30, 2010; , doi: 10.1210/me.2010-0120






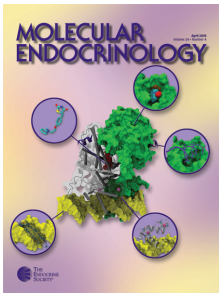

# Glucagon Deficiency Reduces Hepatic Glucose Production and Improves Glucose Tolerance In Adult Mice

Aidan S. Hancock, Aiping Du, Jingxuan Liu, Mayumi Miller, and Catherine L. May

Department of Pathology and Laboratory Medicine (A.S.H., A.D., J.L., M.M., C.L.M.), Children's Hospital of Philadelphia; Department of Pathology and Laboratory Medicine (C.L.M.), University of Pennsylvania School of Medicine; and Institute for Diabetes, Obesity, and Metabolism (C.L.M.), Philadelphia, Pennsylvania 19104

The major role of glucagon is to promote hepatic gluconeogenesis and glycogenolysis to raise blood glucose levels during hypoglycemic conditions. Several animal models have been established to examine the *in vivo* function of glucagon in the liver through attenuation of glucagon via glucagon receptor knockout animals and pharmacological interventions. To investigate the consequences of glucagon loss to hepatic glucose production and glucose homeostasis, we derived mice with a pancreas specific ablation of the $\alpha$-cell transcription factor, *Arx*, resulting in a complete loss of the glucagon-producing pancreatic $\alpha$-cell. Using this model, we found that glucagon is not required for the general health of mice but is essential for total hepatic glucose production. Our data clarifies the importance of glucagon during the regulation of fasting and postprandial glucose homeostasis. **(*Molecular Endocrinology* 24: 1605–1614, 2010)**

Glucagon, the product of pancreatic $\alpha$-cells, is a major counteracting hormone to insulin in regulating glucose homeostasis (1–3). Glucagon promotes hepatic gluconeogenesis and glycogenolysis while inhibiting glycogen synthesis and glycolysis in response to hypoglycemia (4, 5). In addition, glucagon has been shown to play a major role in the development of hyperglycemia in both type 1 and type 2 diabetes mellitus (1–3, 6, 7). As elegantly demonstrated in both man and dog, glucagon plays an important role in the regulation of basal hepatic glucose production (HGP), as well as maintaining glucose levels in the postprandial state (8–12).

Because the development of severe hyperglycemia requires the presence of glucagon, suppressing glucagon action in the liver has been an attractive approach to reverse the metabolic consequences of insulin deficiency. This was first evident when somatostatin, a glucagon suppressant, was shown to restore glucose levels to the normal range in insulin-deficient humans and dogs (6, 10, 13, 14). This observation was further confirmed recently, when the potent glucagon suppressant, leptin, was shown to not only correct the hyperglycemia in the moribund insulin-deficient rodents but also restore the animals to full health (7).

The importance of glucagon signaling in regulating glucose homeostasis has also been demonstrated using genetically modified mouse models and by pharmacological interventions that suppress glucagon activity (15–24). Mice lacking the glucagon receptor (GR) ($Gcgr^{-/-}$) display modest fasting hypoglycemia and improved glucose tolerance, as well as reduced adiposity and circulating triglycerides (16, 18). When challenged with a high-fat diet, $Gcgr^{-/-}$ mice are resistant to obesity and exhibit reduced body weight and improved glucose tolerance (15). In addition, knockdown of GR expression in mice using antisense oligonucleotides (ASOs) lead to improved

ISSN Print 0888-8809 ISSN Online 1944-9917
Printed in U.S.A.

doi: 10.1210/me.2010-0120 Received March 29, 2010. Accepted June 2, 2010.
First Published Online June 30, 2010

Abbreviations: *Arx*, *Aristaless-related homeobox*; ASO, antisense oligonucleotide; CREB, cAMP response element-binding protein; CRTC2, CREB-regulated transcription coactivator 2; FFA, free fatty acid; GIR, glucose infusion rate; GR, glucagon receptor; GTT, glucose tolerance test; H&E, hematoxylin and eosin; HGP, hepatic glucose production; P, postnatal day; PAS, periodic acid-Schiff; P-CREB, phospho-CREB; PEPCK, phosphoenolpyruvate carboxykinase; Rd, glucose disposal rate; STZ, streptozotocin.

glucose metabolism in *ob/ob* mice and decreased HGP (19, 20). Furthermore, high-affinity glucagon neutralizing antibodies, which effectively reduce circulating glucagon, can also lower glucose levels in several animal models (22–24). Recently, it has been reported that although devoid of most, if not all, of the glucagon-derived peptides, *glucagon* null ($Gcg^{gfp/gfp}$) mice are born without gross abnormalities but display lower glucose levels at 2 wk of age (25).

Collectively, there is ample evidence to support the direct link between hyperglucagoniemia and hyperglycemia in diabetes. In this study, we derived mice with a conditional deletion of the X-linked *aristaless-related homeobox* (*Arx*) gene to study the effects of glucagon during HGP and glucose homeostasis. *Arx* has been shown to be the key gene directing endocrine progenitor cells toward the α-cell lineage in the developing pancreas (26–28). *Arx* null animals do not develop α-cells and display severe hypoglycemia shortly after birth (28). Surprisingly, we find that mice with a pancreas-specific deletion of *Arx* have a normal life span despite lack of glucagon-producing α-cells, which is in agreement with what was recently reported in the $Gcg^{gfp/gfp}$ animals (25). This discovery shows that additional defects must be responsible for the perinatal lethality in *Arx* null mice (28). However, adult *Arx*-deficient mice show relative hypoglycemia compared with control animals after fasting and display improved glucose tolerance. Our results confirm and expand what was previously known regarding the role of glucagon during basal and postprandial glucose homeostasis.

## Results

### Derivation of mice deficient for *Arx* in the pancreas

To directly investigate the consequence of a complete loss of glucagon on HGP, glucose homeostasis, and overall health, we derived pancreas-specific *Arx* mutant mice. Mice with a floxed allele of *Arx* (Fig. 1A), $Arx^{fl/fl}$ (29), were bred to mice carrying a transgene with Cre-recombinase under control of the *Pdx1* promoter (30). *Pdx1-Cre;*$Arx^{fl/fl}$ and *Pdx1-Cre;*$Arx^{fl/Y}$ (*Arx* deficient) mice were born at the expected Mendelian distribution and showed no significant differences in size or appearance at any age examined for either gender when compared with littermate controls (data not shown).

To evaluate the specificity and efficiency of Cre-mediated deletion of *Arx*, we first used PCR analysis of genomic DNA to determine whether exon 2 of the *Arx* gene was excised in the pancreas of postnatal d 2 (P)2 *Arx*-deficient mice. Primers were designed to amplify a 402-bp product only detectable when the *Arx* gene was deleted. The PCR analysis using genomic DNA obtained from pancreas and liver indicated that gene ablation occurred only in pancreatic cells of *Arx*-deficient mice and not in liver cells (Fig. 1B). Concordantly, mRNA levels of *Arx* were reduced by approximately 95% in P7 *Arx*-deficient pancreas, whereas no significant differences were detected in the stomach and intestine (Fig. 1C) (data not shown). These data demonstrate that efficient and specific loss of Arx expression in the *Arx*-deficient pancreas is achieved by P7.

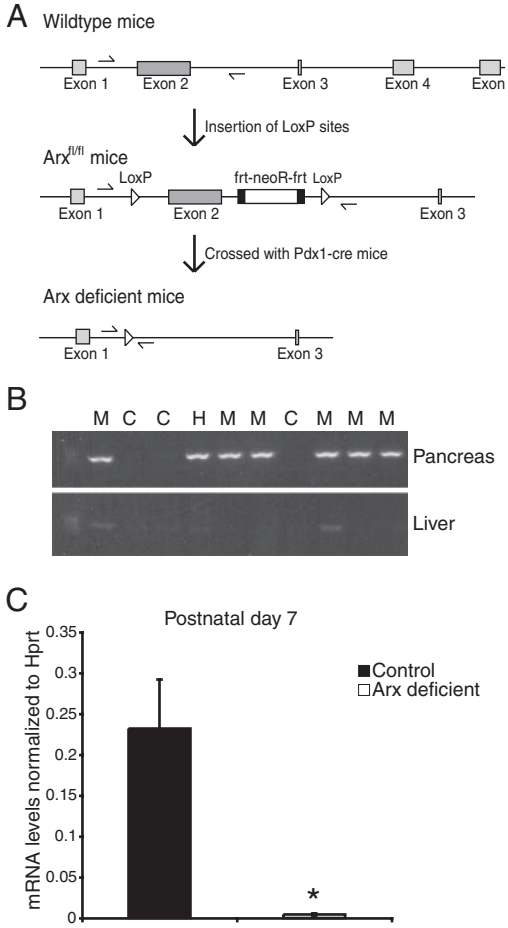


**FIG. 1.** Pdx1-Cre drives pancreas-specific deletion of the *Arx* gene. A, Representation of wild-type gene sequence (*top*) and the insertion of the LoxP sites flanking the exon 2 of the *Arx* gene (*middle*). Removal of exon 2 after crossing the $Arx^{fl/fl}$ mice with *Pdx1-Cre* mice (*bottom*). B, PCR analysis from genomic DNA obtained from pancreas and liver of P2 control (C), heterozygote (H), and *Arx*-deficient mutant (M) animals. Presence of the PCR product (402 bp) indicates efficient ablation of the *Arx* gene in the pancreas but not in the liver. *Arrows* in A indicate the location of the primers used. C, Real-time PCR analysis of *Arx* mRNA levels in P7 control and mutant pancreas. Values are mean ± SEM from three mice per group. *, $P < 0.05$.

### *Arx*-deficient mice display a loss of α-cells and a significant increase in β, δ and PP-cells

To evaluate whether glucagon-producing α-cell differentiation is perturbed in *Arx*-deficient mice, we performed immunohistochemical analysis for glucagon ex-

pression in sections of *Arx*-deficient and control animals at 3–6 months of age. Similarly to what was reported in *Arx* null animals (28), we observed a dramatic reduction in the number of glucagon-producing cells in the *Arx*-deficient pancreas, whereas the number of glucagon-expressing cells in the stomach and intestine were not affected (Fig. 2, A and B, and Supplemental Fig. 1A, published on The Endocrine Society's Journals Online web site at http://mend.endojournals.org) (data not shown). Furthermore, the number of somatostatin-expressing δ-cells and insulin-expressing β-cells was increased within the islets of *Arx*-deficient animals (Fig. 2, C–F). Morphometric analysis confirmed a 99% decrease, as well as 1.5- and 2-fold increases, in the number of glucagon-, insulin-, and somatostatin-producing cells in the pancreas, respectively (Fig. 2, B, D, and F). Interestingly, we also observed an increase in the number of pancreatic peptide-producing PP cells in our *Arx*-deficient mice (Supplemental Fig. 1, B and C), which is in disagreement with what was previously reported in the *Arx* null animals, where a normal number of PP cells was reported (28).

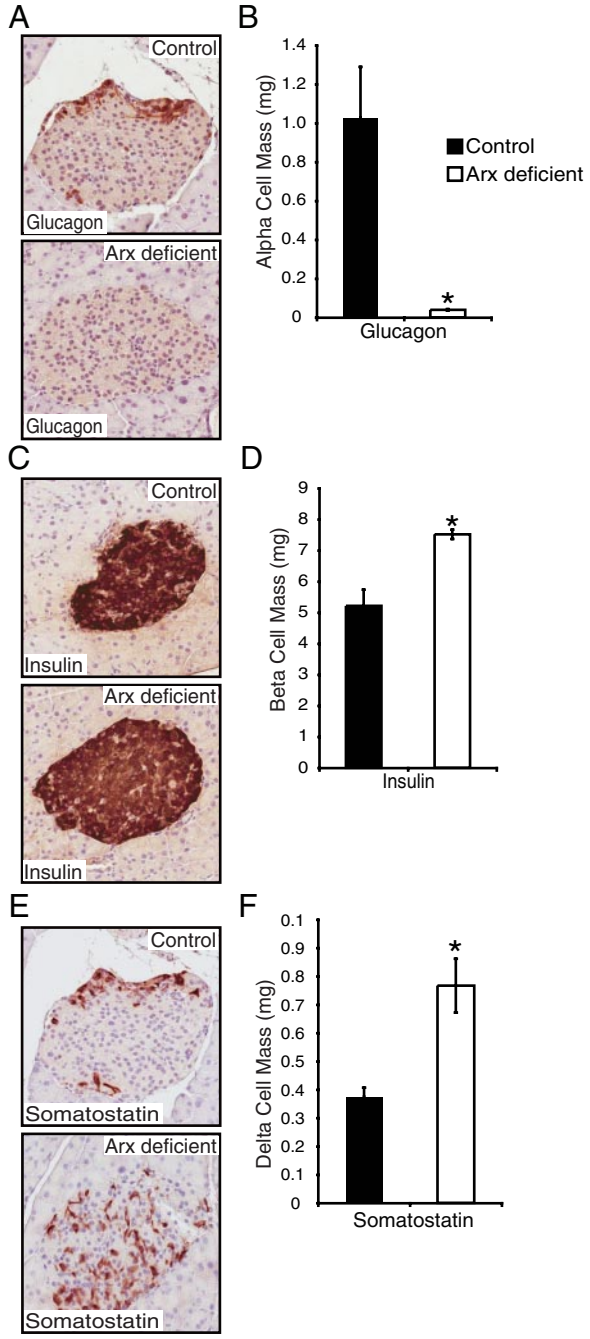


**FIG. 2.** *Arx*-deficient mice lack glucagon-producing cells. A, C, and E, Immunostaining of glucagon, insulin, and somatostatin in 3- to 6-month-old control and *Arx*-deficient pancreas. Morphometric analysis indicated 99% reduction in the α-cell mass (B), 1.5-fold increase in the β-cell mass (D), and 2-fold increase in the δ-cell mass (F) in the *Arx*-deficient animals. Values are mean ± SEM from three mice per group. *, $P < 0.05$ between genotypes.

## *Arx*-deficient mice are healthy with lower fasting blood glucose levels

It has been reported that *Arx* null mice die perinatally (28, 31), and this lethality was attributed to abnormal endocrine function likely resulting in hypoglycemia (28). Strikingly, despite the complete loss of α-cells, our *Arx*-deficient mice were born at the expected Mendelian ratio and are outwardly indistinguishable from control littermates at all ages examined (up to 14 months). Body weights did not differ between the two groups (data not shown). Because glucagon is thought to be critical in maintaining fasting glucose homeostasis, we measured blood glucose levels in both young (6 wk) and older (3–6 month old) *Arx*-deficient mice after 0-, 16-, and 24-h fasts. Although we did not detect a significant difference in glucose levels between *Arx*-deficient and control animals after a 0- or 16-h fast in both age groups (Fig. 3, A and B), the difference in glucose levels did reach significance after the 24-h fast (Fig. 3, A and B). These results suggest that glucagon is required for maintaining normal glucose levels during a prolonged fast regardless of the animals' age.

## *Arx*-deficient mice display improved glucose tolerance test (GTT) with no detectable plasma glucagon

To determine whether glucagon is also critical in maintaining postprandial glucose homeostasis, we performed a GTT on 6-wk-old and 3- to 6-month-old animals. Although we did not observe a difference between *Arx*-deficient and control mice at 6 wk of age (Fig. 3C), we found a significant improvement of glucose tolerance in 3- to 6-month-old *Arx*-deficient mice (Fig. 3D). To determine whether the improved glucose tolerance was associated with the loss of glucagon in the *Arx*-deficient mice, we measured plasma glucagon levels by RIA in 3- to 6-month-old mice after a 16-h fast and found no detectable glucagon in the peripheral blood of *Arx*-deficient

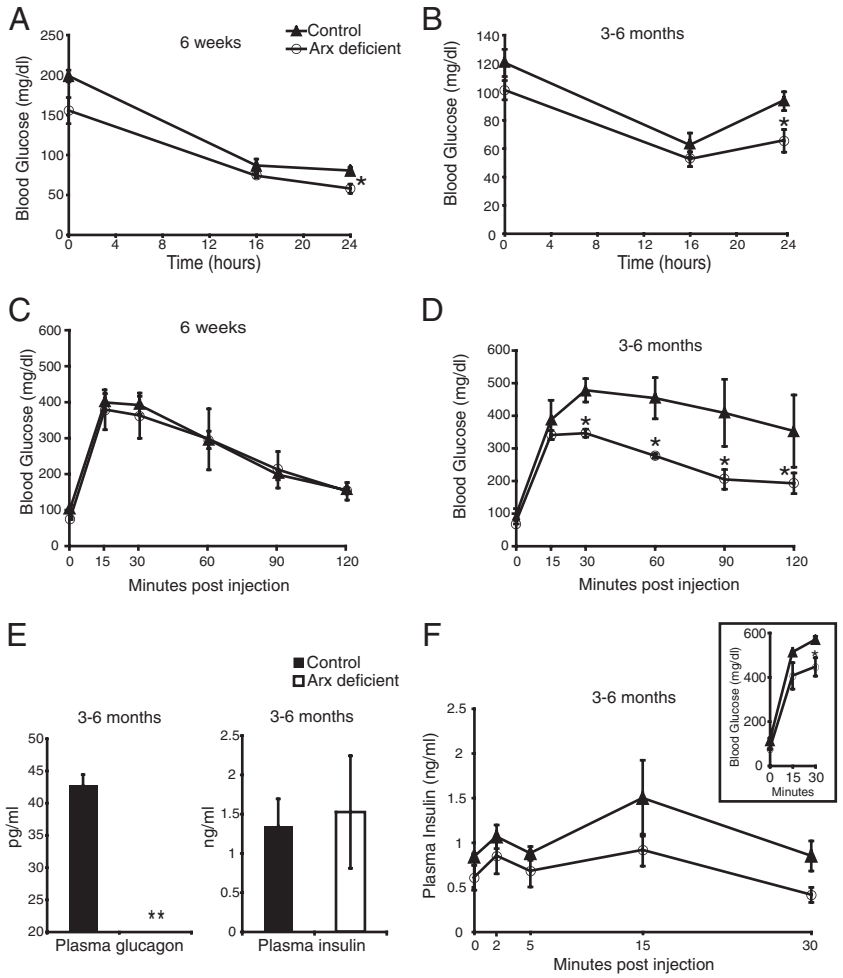


**FIG. 3.** *Arx*-deficient mice have no obvious abnormalities and exhibit improved glucose tolerance with age. A, Blood glucose levels of 6-wk-old male mice after 0-, 16-, or 24-h fast. Values are mean ± SEM from at least three mice per group. *, $P < 0.05$ between genotypes. B, Blood glucose levels of 3- to 6-month-old male mice after 0-, 16-, or 24-h fast. Values are mean ± SEM from at least three mice per group. *, $P < 0.05$ between genotypes. C and D, GTT test of 6-wk-old (C) and 3- to -6-month-old (D) male control and *Arx*-deficient mice. Values are mean ± SEM from at least three mice per group. *, $P < 0.05$ between genotypes. E, Plasma glucagon and insulin levels of 3- to 6-month-old male mice after a 16-h fast. Values are mean ± SEM from four mice per group. *, $P < 0.05$ and between genotypes; **, $P < 0.01$ between genotypes. Plasma glucagon levels fell below detection threshold (20 pg/ml) for *Arx*-deficient animals. F, Plasma insulin levels of 3- to 6-month-old male control and *Arx*-deficient animals was measured during GTT (see *inset*). Values are mean ± SEM from at least three mice per group. *, $P < 0.05$ between genotypes.

animals (Fig. 3E). Interestingly, although we did observe an increase in β-cell mass in the *Arx*-deficient pancreas (Fig. 2, C and D), we did not detect a significant increase of plasma insulin levels in the *Arx*-deficient mice after a 16-h fast (Fig. 3E). To determine whether more insulin is secreted in the *Arx*-deficient mice upon glucose stimulation, we measured the plasma insulin levels during the first 30 min of a GTT in 3- to 6-month-old mice and found no significant increase in insulin secretion from the *Arx*-deficient animals (Fig. 3F). In fact, we noticed a trend of reduced insulin secretion in the *Arx*-deficient mice. These data suggest that the lack of glucagon contributes to the improved glucose tolerance in adult *Arx*-deficient mice.

### *Arx*-deficient mice have reduced HGP

Glucagon helps to maintain blood glucose levels by promoting glycogenolysis and gluconeogenesis, resulting in increased HGP. To assess whether glucose production in the *Arx*-deficient animals was affected, we performed a hyperinsulinemic/euglycemic clamp study on 2-month-old mice while the blood glucose levels were mantained between 60–70 mg/dl (control, 64.1 ± 2.6 mg/dl; and mutant, 64.9 ± 2.1 mg/dl). Although there was no difference in the glucose disposal rate (Rd), the glucose infusion rate (GIR) trended higher in *Arx*-deficient animals, suggesting that more glucose was needed to keep the blood glucose levels steady. This would only occur if there was lower HGP, which was indeed evident in our *Arx*-deficient mice (Fig. 4A). These data demonstrate that glucagon deficiency results in reduced HGP in *Arx*-deficient mice.

### *Arx*-deficient mice have increased quantities of glycogen in the liver

Next, to determine whether there are histological differences in the liver of the *Arx*-deficient mice, we compared hematoxylin and eosin (H&E) stained sections from 3- to 6-month-old control and *Arx*-deficient mice. Although there were no gross morphological differences in the liver between control and *Arx*-deficient animals (Fig. 4B), glycogen granules were clearly larger and more plentiful in *Arx*-deficient mice, suggesting that lack of glucagon results in accumulation of glycogen in the liver (Fig. 4B). Periodic acid-Schiff (PAS) staining, which labels glycogen granules in the liver, further confirmed the presence of increased glycogen in the *Arx*-deficient liver (Fig. 4D). Furthermore, hepatic glycogen content in the *Arx*-deficient mice was also significantly increased (Fig. 4C). These data suggest that in the absence of glucagon production, enhanced glycogen synthesis or suppressed hepatic glycogenolysis occur in the liver of *Arx*-deficient mice, resulting in excess glycogen granules.

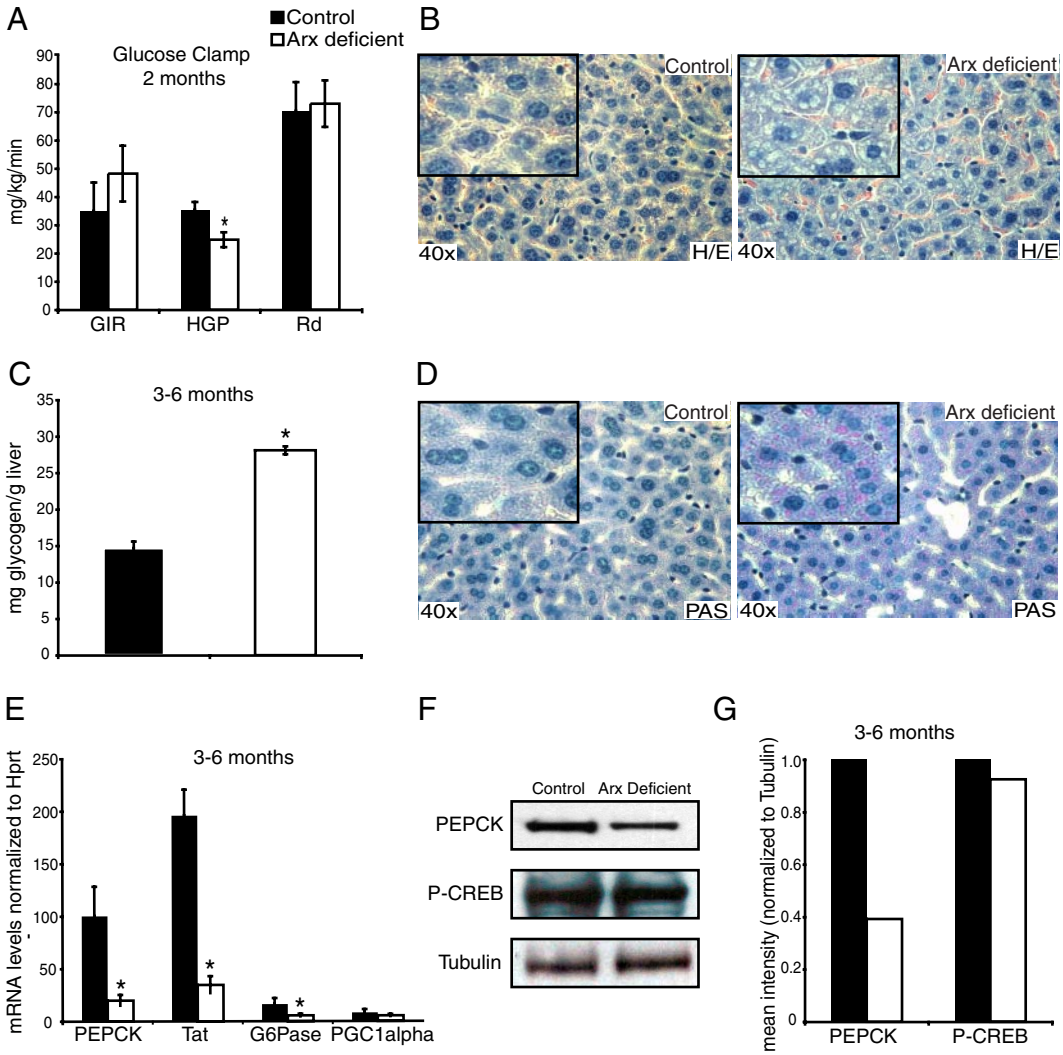


**FIG. 4.** *Arx*-deficient mice exhibit increased fat and glycogen in the liver. A, GIR HGP, and Rd were measured during the clamp from 2-month-old male control and *Arx*-deficient mice. Values are mean ± SEM from five mice per group. *, $P < 0.05$ between genotypes. B, Liver histology of 3- to 6-month-old male control and *Arx*-deficient paraffin-embedded liver sections stained with H&E or (D) Periodic acid-Schiff (PAS) (magnification, ×40). An *enlarged portion of the image* is provided in the *box*. C, Glycogen levels were measured in liver taken from mice at 3–6 months of age after a 16-h fast. Values are mean ± SEM from three mice per group. *, $P < 0.05$ between genotypes. E, Real-time PCR analysis measured relative mRNA levels of genes involved in gluconeogenesis from 3- to 6-month-old male after a 16-h fast. Tat, Tyrosine amino transferase. Values are mean ± SEM from four mice per group. *, $P < 0.05$ between genotypes. F, Western blot analysis using liver samples of 3- to 6-month-old male control and *Arx*-deficient animals to detect PEPCK (63 kDa), P-CREB (43 kDa), and tubulin (50 kDa). G, Mean intensity of PEPCK and P-CREB normalized to tubulin as quantified from Western blot analysis.

## mRNA levels of major gluconeogenic genes are down-regulated in fasted *Arx*-deficient mice

To investigate whether hepatic gluconeogenesis is impaired in *Arx*-deficient mice, we next examined the expression of genes involved during this process by quantitative PCR analysis. We found that mRNA levels of *phosphoenolpyruvate carboxykinase* (*PEPCK*) (70% reduction) *tyrosine amino transferase* (76% reduction), and *glucose 6 phosphotase* (60% reduction) were significantly down-regulated in the *Arx*-deficient liver after a 16-h fast (Fig. 4E). Levels of *peroxisome proliferators-activated receptor-γ coactivator 1α* mRNA were also reduced, although not statistically significant (Fig. 4E). Furthermore, the level of PEPCK protein was reduced by 60% in *Arx*-deficient mice (Fig. 4, F and G). Thus, as expected, expression of genes involved in hepatic gluconeogenesis was impaired in the absence of glucagon. Interestingly, levels of phospho-cAMP response element-binding protein (P-CREB) were unchanged in the *Arx*-deficient liver, in agreement with recent findings that glucagon action is mediated by the CREB coactivator CREB-regulated transcription coactivator 2 (CRTC2) and is independent of CREB phosphorylation (28, 32–34). These results suggest that during a 16-h fast, glucagon is required to fully activate gluconeogenic genes in the liver to promote glucose production. To determine whether other fight-or-flight hormones, *i.e.* catecholamines, were increased in the *Arx*-defi-

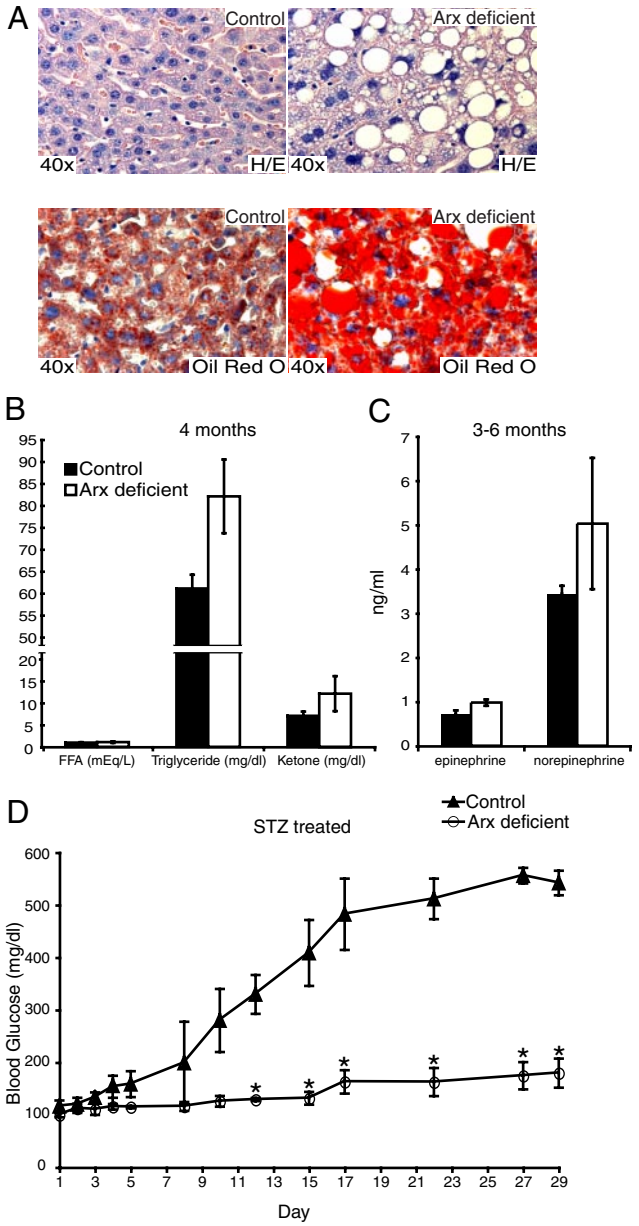


**FIG. 5.** Liver histology from 1-yr-old control and *Arx*-deficient mice. A, H&E and Oil red O staining of 1-yr-old control and *Arx*-deficient mice. B, Plasma lipid profile of 4-month-old control and *Arx*-deficient animals after a 16-h fast. C, Plasma epinephrine and norepinephrine levels of 3- to 6-month-old mice after a 16-h fast. D, Blood glucose levels measured during and after STZ treatment. Day 1–5 was measured after a 4-h fast, d 6 onwards was measured after a 1-h fast. Values are mean ± SEM from at least three mice per group. *, $P < 0.05$ between genotypes.

cient animals to maintain glucose homeostasis, we next measured both epinephrine and norepinephrine and detected an increase, although not statistically significant, in *Arx*-deficient mice (Fig. 5C).

### *Arx*-deficient mice have higher fat content in the liver

In addition to the increased number of glycogen granules in the *Arx*-deficient liver (Fig. 4, B and D), we noticed large vacuoles in the hepatocytes of *Arx*-deficient mice (Fig. 5A). We confirmed the presence of excess lipid droplets in the liver sections of the *Arx*-deficient mice by Oil red O staining (Fig. 5A). At the same time, plasma triglyceride and ketone levels were both increased in *Arx*-deficient mice, although not statistically significant (Fig. 5B).

### *STZ*-treated *Arx*-deficient mice exhibit improved blood glucose

Excess levels of circulating glucagon lead to overproduction of hepatic glucose, which in turn contributes to the severe hyperglycemia observed in diabetic patients. To investigate whether endogenous hyperglycemia can be eliminated in our *Arx*-deficient mice, devoid of glucagon-producing α-cells, we next treated both control and *Arx*-deficient mice with the β-cell toxin streptozotocin (STZ) (35). After treating mice with STZ, we measured glucose levels every other day for 24 d in both control and *Arx*-deficient mice. Monitoring of the blood glucose levels in control mice revealed that the β-cells were efficiently ablated by the STZ treatment, because these mice began to display elevated glucose levels as early as 1 wk after treatment onset. The control mice, within 2 wk of STZ treatment, were severely diabetic with blood glucose levels more than 350 mg/dl (Fig. 5D). Unlike controls, blood glucose levels of STZ-treated *Arx*-deficient mice remained between 100 and 180 mg/dl at all time points examined (Fig. 5D). These data suggest that the diabetes resulting from β-cell deficiency is glucagon-dependent in mice, just as had been seen in dog and man (6, 10, 13, 14).

## Discussion

For the past 35 yr, the action of glucagon has been investigated using potent glucagon suppressors and by targeting the GR via genetic ablation, ASOs, and neutralizing antibodies (6, 10, 13, 14, 16, 21, 25). Recently, glucagon null ($Gcg^{gfp/gfp}$) animals have been reported that display improved glycemic control and hyperplasisa of islet α-cells, but these mice do not allow to separate the effects of GLP1 and GLP2, also produced from the glucagon gene, from those of glucagon itself (25). In this study, we have derived mice lacking pancreatic α-cells to address the requirement for glucagon in the normal life of an animal and regulation of glucose homeostasis. It has previously been shown that *Arx* null mice exhibit perinatal lethality, which was attributed to anomalous endocrine pancreatic function, because *Arx* null mice show severe hypoglycemia 2 d after birth (26, 28). To our surprise, despite the complete loss of glucagon-producing cells in the pancreas and no detectable circulating blood glucagon, *Arx*-deficient animals are born alive and have a normal life span, which is similar to what was reported in the

*Gcg*$^{gfp/gfp}$ animals (25). The findings presented above suggest that the cause of death is independent of the loss of glucagon-producing cells in the *Arx* null animals. In addition, reports from others have suggested that *Arx* null mice likely die from either seizures and/or olfactory bulb defects, caused by *Arx* deficiency in the brain (29, 31). Furthermore, we have detected an increase of catecholamines levels in the *Arx*-deficient animals, indicating that other stress hormones are likely to compensate for the loss of glucagon in *Arx*-deficient mice allowing normal growth and development.

Although we detected a modest increase in β-cell mass in the *Arx*-deficient mice, we did not observe a significant increase in circulating blood insulin levels after a 16-h fast. This would suggest that the slightly reduced levels of basal glucose seen in the *Arx*-deficient animals are caused by the absence of glucagon and are not due to an increase in circulating insulin levels. Furthermore, we detected an improvement of postprandial glucose homeostasis in the *Arx*-deficient mice. However, this change was not evident until the animals reached 3–6 months of age. Although it is not clear why we did not observe a difference in the GTT in 6-wk-old *Arx*-deficient and control animals, the likely explanation is the involvement of other hormones in these young animals. Interestingly, although not statistically significant, we did notice a trend of reduced insulin secretion during the first 30 min of a GTT in the *Arx*-deficient animals. However, the exact cause of this reduction remained to be further investigated, although this is likely the consequence of lower glucose levels in our mutant mice. Lastly, we have also observed an increase in the number of somatostatin-producing and pancreatic polypeptide-producing cells and their distribution throughout the medulla of the islet. The increase of δ-cells in our *Arx*-deficient animals is reminiscent of what was reported in the *Arx* null animals due to the critical role of Arx in repressing δ-cell lineage in the developing pancreas (26, 28). Together with the increased levels of plasma catecholamines and the increase number of somatostatin-producing cells in the *Arx*-deficient animals, endogenous insulin release might be dampened (36). However, this possibility remains to be investigated further. In contrast, it is unclear why the number of PP cells was increased in the mantle of the islets and why some insulin-expressing cells also coexpress pancreatic polypeptide in our *Arx*-deficient animals. These findings in our *Arx*-deficient mice are different from what was reported in the *Arx* null mice, where normal numbers of PP cells were found (26, 28). This discrepancy might due to the timing of *Arx* ablation in the developing pancreas, suggesting that there might be a critical window that *Arx* acts in controlling PP cell lineage.

It has recently been shown that PEPCK, one of the key enzymes regulating gluconeogenesis, alone only has a weak influence during this process (37, 38). In our *Arx*-deficient animals, we found reduced expression of genes regulating hepatic gluconeogenesis, including a 60% reduction in the PEPCK protein levels. Burgess *et al*. (37) showed that the protein levels of PEPCK have to be reduced by 80% or more before any effects are observed. However, the lack of glucagon in our mice impacts the expression of several gluconeogenic genes other than PEPCK, which likely collectively affect glucose production.

It has been demonstrated by several studies that upon glucagon stimulation, CRTC2, a cofactor of CREB, gets dephosphorylated, then translocates into the nucleus, and forms transcriptional complexes with P-CREB to activate gluconeogenesis in the liver (32–34, 39). The sustained levels of P-CREB, in our *Arx*-deficient mice, further strengthens the importance of glucagon for CRTC2 recruitment in initiating hepatic gluconeogenesis, which is independent of CREB phosphorylation.

Although the *Arx*-deficient, *Gcg*$^{gfp/gfp}$, *Gcgr*$^{-/-}$, and GR-ASO-treated mice all exhibit lower blood glucose and improved glucose tolerance, *Gcg*$^{gfp/gfp}$, *Gcgr*$^{-/-}$, and GR-ASO mice have additional phenotypes not present in the *Arx*-deficient mice. For instance, *Gcgr*$^{-/-}$ and GR-ASO-treated mice display supraphysiological levels of glucagon, and α-cell hyperplasia was observed in the *Gcg*$^{gfp/gfp}$ and *Gcgr*$^{-/-}$ mice (16, 19, 20, 25). Similar to our *Arx*-deficient mice, mRNA levels of several gluconeogenic and glycogenolytic enzymes were decreased in the GR-ASO-treated mice (19). Furthermore, mice deficient in prohormone convertase 2, which lack mature α-cells, also display lower blood glucose levels, α-cell hyperplasia, and improved glucose tolerance similar to the *Gcgr*$^{-/-}$ mice (21, 40). However, interpretation of this model is complicated by the fact that prohormone convertase 2 is also required for processing of other endocrine hormones (40, 41). Finally, it was recently reported that ectopic expression of paired box gene 4 in the mouse pancreas results in overproduction of insulin-secreting β-cells at the expense of α-cells, and these transgenic mice display improved glucose tolerance and increase in plasma insulin levels at 3 wk of age (42).

During a prolonged fast, the body activates both HGP and ketogenesis. Ketogenesis is fueled by an increase in free fatty acid (FFA) levels resulting from lipolysis in adipose tissue, which is no longer suppressed by insulin. However, because FFA levels were not elevated in the *Arx*-deficient mice, one of the likely explanations for the excess glycogen and fat in the liver of *Arx*-deficient mice is lack of glucagon, which results in enhanced hepatic

glucose entry and overaccumulation of carbon to be stored as glycogen and fat. Furthermore, the relative hypoglycemia in our *Arx*-deficient mice could potentially cause a small increase in the rate of lipolysis, thus compensating for the loss of glucagon stimulation, maintaining FFA levels at normal levels. At the same time, the rate of ketogenesis may have had a small increase caused by the slight hypoglycemia, thus increasing the conversion of FFA to ketone bodies. Elevated levels of epinephrine and norepinephrine would also stimulate this. In addition, limitation of the assay, mixed background of the animals, and the number of animals used may have prevented us from observing a sustained increase of FFA levels.

In this study, we have derived and analyzed one of the first mouse models with a complete ablation of α-cells in the adult pancreas to directly study the impact of glucagon during basal and postprandial glucose homeostasis. We have demonstrated that although glucagon is critical during a prolonged fast and postprandial glucose homeostasis, it is not essential for the health of an animal. Our results have extended the role of glucagon in regulating glucose homeostasis and provided further evidence that glucagon suppression or elimination can limit the consequences of insulin deficiency in diabetes.

## Materials and Methods

### Animals and breeding strategy

The derivation of the $Arx^{fl/fl}$ and *Pdx1-Cre* transgenic line has been reported previously (29, 30). All mice were kept on a mixed background. $Arx^{fl/Y}$ and $Arx^{fl/+}$;*Pdx1-Cre* mice were mated to generate $Arx^{fl/fl}$;*Pdx1-Cre* or $Arx^{fl/Y}$;*Pdx1-Cre* mutant mice. Littermate heterozygous mice were indistinguishable from control animals. The Children's Hospital of Philadelphia's Institutional Animal Care and Use Committee approved all animal experiments.

### GTTs and analytical procedures

Overnight fasted animals were injected ip with 2 g of glucose (Sigma, St. Louis, MO) per kilogram of body weight. Blood glucose values were monitored at 0, 15, 30, 60, 90, and 120 min after injection using an automatic glucometer (One Touch Ultra; LifeScan, Milpitas, CA). For hormone/lipid measurement, blood was collected in heparinized tubes (BD Microtainer, BD, Franklin Lakes, NJ) spun and stored at −20 C until assayed. Plasma insulin was measured using ELISA assay. Plasma lipid levels were measured by the Mouse Phenotyping, Physiology, and Metabolism Core at University of Pennsylvania. For plasma glucagon measurements, after blood collection, 250 KIU/ml of aprotinin was added to 200 μl of whole blood to preserve the glucagon proteins from degradation. Samples were then spun in heparinized tubes, and 100 μl of plasma was snap frozen. Final concentration of aprotinin was 500 KIU/ml. Plasma glucagon levels were then measured using a RIA by the RIA/Biomarkers core at University of Pennsylvania. Epinephrine and norepinephrine levels were measured using 2-CAT (A-N) Research Elisa (BA E-5400; LDN, Nordhorn, Germany) according to manufacture's instructions. Specifically, EDTA (final concentration, 1 mM) and sodium metabisulfite (final concentration, 4 mM) were added to the whole blood to prevent degradation.

### Histology

Tissues were fixed in 4% paraformaldehyde, then embedded in paraffin. Slides (7-μm sections) were cut, then deparaffinized. Primary antibodies were glucagon (1:3000; Millipore, Billerica, MA), insulin (1:1000; Millipore), PP (1:50; Invitrogen, Carlsbad, CA), and somatostatin (1:3000; Santa Cruz Biotechnology, Inc., Santa Cruz, CA). The sections were then incubated with either a fluorescent secondary antibody (1:600) or a biotinylated secondary antibody (1:200). The biotinylated antibody was followed by incubation with the ABC elite reagent and color reaction using the diaminobenzidine substrate kit according to the recommendation from the manufacturer (Vector Laboratories, Burlingame, CA). After the color reaction, sections were dehydrated and mounted with histomount (Invitrogen). Sections were counterstained for H&E before dehydration to help visualize the tissue morphology. Slides were then given to the Children's Hospital of Philadelphia pathology core for slide scanning. PAS staining on deparaffinized liver sections (6 μm) was done by placing the slides sequentially in 0.5% periodic acid solution, Schiff reagent, hematoxylin, 0.5% acid alcohol, and saturated lithium carbonate. Oil red O staining was performed using frozen liver tissue.

### Quantitative PCR analysis

Tissues were homogenized in TRIzol reagent. The RNA was recovered by chloroform extraction and then purified using RNeasy mini kit (QIAGEN, Germantown, MD). RNA was reverse-transcribed using 0.5 μg Oligo (dT) primer, Superscript II Reverse Transcriptase, and accompanying reagents (Invitrogen). Real-time PCR reactions were set up using the Brilliant SYBR Green PCR Master Mix (Stratagene, La Jolla, CA). All reactions were performed in triplicate with reference dye normalization and median cycling threshold values used for analysis. Primer sequences are available upon request.

### α-, β-, And δ-cell mass

Pancreata of male 3- to 6-month-old control and mutant mice was removed, weighed, fixed in 4% paraformaldehyde overnight at 4 C, and embedded in paraffin. Sections (7 μm) with maximum footprint were used for insulin, glucagon, and somatostatin immunostaining. Images were taken under ×4 magnification, and pancreatic tissue positive for insulin, glucagon, and somatostatin staining were measured using Aperio software. Cell mass was obtained by measuring the fraction of strong positive pixels to total tissue area and multiplying by the pancreatic weight. Three sections were used per pancreas with three control and mutant pancreata analyzed.

### Hyperinsulinemic-euglycemic clamp

An indwelling catheter was inserted in the right internal jugular vein under sodium pentobarbital anesthesia and extended to the right atrium. After a 6-h fast, a 120-min hyperinsulinemic-euglycemic clamp was conducted with a continuous infusion of human insulin (Humulin; Novo Nordisk, Princeton, NJ) at a rate of 2.5 mU/kg·min to raise plasma insulin within a physiological range. Tail blood samples (20 μl) were collected at 10- to 20-min intervals for the immediate measurement of

plasma glucose concentration, and 20% glucose was infused at variable rates to maintain plasma glucose at basal concentrations. Blood glucose was sustained at 60–70 mg/dl, and glucose levels were checked every 10 min during the procedure to ensure a steady state. Insulin-stimulated whole-body glucose flux was estimated using a prime-continuous infusion of HPLC-purified [3-$^3$H]glucose (10 $\mu$Ci bolus, 0.1 $\mu$Ci/min; PerkinElmer Life and Analytical Sciences, Boston, MA) throughout the clamps. To estimate insulin-stimulated glucose transport activity in individual tissues, 2-deoxy-D-[1-$^{14}$C]glucose (2-[$^{14}$C]DG; PerkinElmer Life and Analytical Sciences) was administered as a bolus (10 $\mu$Ci) at 45 min before the end of clamps. Blood samples (20 $\mu$l) were taken at 77, 80, 85, 90, 100, 110, and 120 min after the start of clamps for the determination of plasma [$^3$H]glucose, $^3H_2O$, and 2-[$^{14}$C]DG concentrations. Additional blood samples (10 $\mu$l) were collected before the start and at the end of clamps for measurement of plasma insulin concentrations. All infusions were done using a Programmable Syringe Pump BS-8000 (Braintree Scientific, Inc., Braintree, MA). The rates of basal glucose turnover and whole-body glucose uptake are measured as the ratio of [$^3$H] GIR (dpm) to the specific activity of plasma glucose. HGP during clamp is measured by subtracting the GIR from the whole-body glucose uptake (Rd).

### STZ treatment

Diabetes was induced by ip injection of STZ (50 mg/kg body weight; Sigma-Aldrich, St. Louis, MO) for five consecutive days after a 4-h fast. Blood glucose measurements for d 1–5 were performed after a 4-h fast. Blood glucose levels from d 6 onwards were performed after a 1-h fast.

### Hepatic glycogen content

One hundred milligrams of frozen liver samples were homogenized in 6% perchloric acid and then mixed with 100 $\mu$g amyloglucosidase (Sigma) for 2 h. Glucose was measured using the Amplex Red kit (Invitrogen).

### Western blot analysis

Protein from small liver sections was extracted by repeatedly freezing/thawing the sample, then homogenizing the remaining tissue followed by a final sonication step; 20 $\mu$g/lane of the extract was separated by 10% SDS-PAGE and subsequently transferred to a nitrocellulose membrane. This assay was performed using mouse monoclonal tubulin antibody (Sigma), rabbit polyclonal P-CREB antibody (Cell Signaling, Danvers, MA), or rabbit polyclonal PEPCK antibody (Cayman Chemical Co., Ann Arbor, MI). Analysis of the resulting blot was performed using mean intensity of P-CREB or PEPCK normalized to tubulin.

### Statistical analysis

All error bars represent SEM, calculated by dividing the SD of each group by the square root of n. A *t* test was performed to measure significance.

## Acknowledgments

We thank Dr. Klaus Kaestner for careful reading of the manuscript; Dr. Swain, Jaclyn Twaddle, and the members of the Morphology Core in the Center for Molecular Studies in Digestive and Liver Disease (P30-DK050306); Dr. Heather Collins of the RIA/Biomarkers and Dr. Ravindra Dhir of the Mouse Phenotyping, Physiology and Metabolism Cores of the Penn Diabetes Center (P30-DK19525) for sample processing; Dr. Jeff Golden for the *Arx* floxed mice; Dr. Pedro Herrera for the *Pdx1-Cre* mice; and Dr. John Le Lay for his technical assistance and discussions.

Address all correspondence and requests for reprints to: Catherine L. May, Department of Pathology and Laboratory Medicine, Children's Hospital of Philadelphia, 3615 Civic Center Boulevard, Room 516E, Philadelphia, Pennsylvania 19104. E-mail: catheril@mail.med.upenn.edu.

This work was supported by National Institutes of Health Grants NIH-DK078606, NIH-DK019525, and Juvenile Diabetes Research Foundation 2-2007-703 (to C.L.M.).

Disclosure Summary: The authors have nothing to disclose.

## References

1. **Unger RH** 1971 Glucagon and the insulin: glucagon ratio in diabetes and other catabolic illnesses. Diabetes 20:834–838
2. **Burcelin R, Katz EB, Charron MJ** 1996 Molecular and cellular aspects of the glucagon receptor: role in diabetes and metabolism. Diabetes Metab 22:373–396
3. **Toft I, Gerich JE, Jenssen T** 2002 Autoregulation of endogenous glucose production during hyperglucagonemia. Metabolism 51:1128–1134
4. **Jiang G, Zhang B** 2003 Glucagon and regulation of glucose metabolism. Am J Physiol Endocrinol Metab 284:671–678
5. **Consoli A** 1992 Role of liver in pathophysiology of NIDDM. Diabetes Care 15:430–441
6. **Dobbs R, Sakurai H, Sasaki H, Faloona G, Valverde I, Baetens D, Orci L, Unger R** 1975 Glucagon: role in the hyperglycemia of diabetes mellitus. Science 187:544–547
7. **Yu X, Park BH, Wang MY, Wang ZV, Unger RH** 2008 Making insulin-deficient type 1 diabetic rodents thrive without insulin. Proc Natl Acad Sci USA 105:14070–14075
8. **Cherrington AD, Lacy WW, Chiasson JL** 1978 Effect of glucagon on glucose production during insulin deficiency in the dog. J Clin Invest 62:664–677
9. **Holste LC, Connolly CC, Moore MC, Neal DW, Cherrington AD** 1997 Physiological changes in circulating glucagon alter hepatic glucose disposition during portal glucose delivery. Am J Physiol 273:E488–E496
10. **Liljenquist JE, Bloomgarden ZT, Cherrington AD, Perry JM, Rabin D** 1979 Possible mechanism by which somatostatin-induced glucagon suppression improves glucose tolerance during insulinopaenia in man. Diabetologia 17:139–143
11. **Liljenquist JE, Mueller GL, Cherrington AD, Keller U, Chiasson J-L, Perry JM, Lacy WW, Rabinowitz D** 1977 Evidence for an important role of glucagon in the regulation of hepatic glucose production in normal man. J Clin Invest 59:369–374
12. **Shah P, Vella A, Basu A, Basu R, Schwenk WF, Rizza RA** 2000 Lack of suppression of glucagon contributes to postprandial hyperglycemia in subjects with type 2 diabetes mellitus. J Clin Endocrinol Metab 85:4053–4059
13. **Gerich JE, Lorenzi M, Bier DM, Schneider V, Tsalikian E, Karam JH, Forsham PH** 1975 Prevention of human diabetic ketoacidosis by somatostatin. Evidence for an essential role of glucagon. N Engl J Med 292:985–989
14. **Raskin P, Unger RH** 1978 Hyperglucagonemia and its suppression. Importance in the metabolic control of diabetes. N Engl J Med 299:433–436
15. **Conarello SL, Jiang G, Mu J, Li Z, Woods J, Zycband E, Ronan J, Liu F, Roy RS, Zhu L, Charron MJ, Zhang BB** 2007 Glucagon

receptor knockout mice are resistant to diet-induced obesity and streptozotocin-mediated β cell loss and hyperglycaemia. Diabetologia 50:142–150

16. **Gelling RW, Du XQ, Dichmann DS, Romer J, Huang H, Cui L, Obici S, Tang B, Holst JJ, Fledelius C, Johansen PB, Rossetti L, Jelicks LA, Serup P, Nishimura E, Charron MJ** 2003 Lower blood glucose, hyperglucagonemia, and pancreatic α cell hyperplasia in glucagon receptor knockout mice. Proc Natl Acad Sci USA 100: 1438–1443
17. **Sinclair EM, Yusta B, Streutker C, Baggio LL, Koehler J, Charron MJ, Drucker DJ** 2008 Glucagon receptor signaling is essential for control of murine hepatocyte survival. Gastroenterology 135: 2096–2106
18. **Sørensen H, Winzell MS, Brand CL, Fosgerau K, Gelling RW, Nishimura E, Ahren B** 2006 Glucagon receptor knockout mice display increased insulin sensitivity and impaired β-cell function. Diabetes 55:3463–3469
19. **Sloop KW, Cao JX, Siesky AM, Zhang HY, Bodenmiller DM, Cox AL, Jacobs SJ, Moyers JS, Owens RA, Showalter AD, Brenner MB, Raap A, Gromada J, Berridge BR, Monteith DK, Porksen N, McKay RA, Monia BP, Bhanot S, Watts LM, Michael MD** 2004 Hepatic and glucagon-like peptide-1-mediated reversal of diabetes by glucagon receptor antisense oligonucleotide inhibitors. J Clin Invest 113:1571–1581
20. **Liang Y, Osborne MC, Monia BP, Bhanot S, Gaarde WA, Reed C, She P, Jetton TL, Demarest KT** 2004 Reduction in glucagon receptor expression by an antisense oligonucleotide ameliorates diabetic syndrome in db/db mice. Diabetes 53:410–417
21. **Parker JC, Andrews KM, Allen MR, Stock JL, McNeish JD** 2002 Glycemic control in mice with targeted disruption of the glucagon receptor gene. Biochem Biophys Res Commun 290:839–843
22. **Brand CL, Jørgensen PN, Knigge U, Warberg J, Svendsen I, Kristensen JS, Holst JJ** 1995 Role of glucagon in maintenance of euglycemia in fed and fasted rats. Am J Physiol 269:E469–477
23. **Brand CL, Jørgensen PN, Svendsen I, Holst JJ** 1996 Evidence for a major role for glucagon in regulation of plasma glucose in conscious, nondiabetic, and alloxan-induced diabetic rabbits. Diabetes 45:1076–1083
24. **Brand CL, Rolin B, Jørgensen PN, Svendsen I, Kristensen JS, Holst JJ** 1994 Immunoneutralization of endogenous glucagon with monoclonal glucagon antibody normalizes hyperglycaemia in moderately streptozotocin-diabetic rats. Diabetologia 37:985–993
25. **Hayashi Y, Yamamoto M, Mizoguchi H, Watanabe C, Ito R, Yamamoto S, Sun XY, Murata Y** 2009 Mice deficient for glucagon gene-derived peptides display normoglycemia and hyperplasia of islet a-cells but not of intestinal L-cells. Mol Endocrinol 23:1990–1999
26. **Collombat P, Hecksher-Sørensen J, Broccoli V, Krull J, Ponte I, Mundiger T, Smith J, Gruss P, Serup P, Mansouri A** 2005 The simultaneous loss of Arx and Pax4 genes promotes a somatostatin-producing cell fate specification at the expense of the α- and β-cell lineages in the mouse endocrine pancreas. Development 132:2969–2980
27. **Collombat P, Hecksher-Sørensen J, Krull J, Berger J, Riedel D, Herrera PL, Serup P, Mansouri A** 2007 Embryonic endocrine pancreas and mature β cells acquire α and PP cell phenotypes upon Arx misexpression. J Clin Invest 117:961–970
28. **Collombat P, Mansouri A, Hecksher-Sorensen J, Serup P, Krull J, Gradwohl G, Gruss P** 2003 Opposing actions of Arx and Pax4 in endocrine pancreas development. Genes Dev 17:2591–2603
29. **Marsh E, Fulp C, Gomez E, Nasrallah I, Minarcik J, Sudi J, Christian SL, Mancini G, Labosky P, Dobyns W, Brooks-Kayal A, Golden JA** 2009 Targeted loss of Arx results in a developmental epilepsy mouse model and recapitulates the human phenotype in heterozygous females. Brain 132:1563–1576
30. **Herrera PL** 2000 Adult insulin- and glucagon-producing cells differentiate from two independent cell lineages. Development 127: 2317–2322
31. **Kitamura K, Yanazawa M, Sugiyama N, Miura H, Iizuka-Kogo A, Kusaka M, Omichi K, Suzuki R, Kato-Fukui Y, Kamiirisa K, Matsuo M, Kamijo S, Kasahara M, Yoshioka H, Ogata T, Fukuda T, Kondo I, Kato M, Dobyns WB, Yokoyama M, Morohashi K** 2002 Mutation of ARX causes abnormal development of forebrain and testes in mice and X-linked lissencephaly with abnormal genitalia in humans. Nat Genet 32:359–369
32. **Le Lay J, Tuteja G, White P, Dhir R, Ahima R, Kaestner KH** 2009 CRTC2 (TORC2) contibutes to the transcriptional response to fasting in the liver but is not required for the maintenance of glucose homeostasis. Cell Metabolism 10:55–62
33. **Wang Y, Inoue H, Ravnskjaer K, Viste K, Miller N, Liu Y, Hedrick S, Vera L, Montminy M** 2010 Targeted disruption of the CREB coactivator Crtc2 increases insulin sensitivity. Proc Natl Acad Sci USA 107:3087–3092
34. **Wang Y, Vera L, Fischer WH, Montminy M** 2009 The CREB coactivator CRTC2 links hepatic ER stress and fasting gluconeogenesis. Nature 460:534–537
35. **Okamoto H** 1985 The role of poly(ADP-ribose) synthetase in the development of insulin-dependent diabetes and islet B-cell regeneration. Biomed Biochim Acta 44:15–20
36. **Koerker DJ, Ruch W, Chideckel E, Palmer J, Goodner CJ, Ensinck J, Gale CC** 1974 Hypothalamic inhibitor of the endocrine pancreas. Science 184:482–484
37. **Burgess SC, He T, Yan Z, Lindner J, Sherry AD, Malloy CR, Browning JD, Magnuson MA** 2007 Cytosolic phosphoenolpyruvate carboxykinase does not solely control the rate of hepatic gluconeogenesis in the intact mouse liver. Cell Metab 5:313–320
38. **Edgerton DS, Ramnanan CJ, Grueter CA, Johnson KM, Lautz M, Neal DW, Williams PE, Cherrington AD** 2009 Effects of insulin on the metabolic control of hepatic gluconeogenesis in vivo. Diabetes 58:2766–2775
39. **He L, Sabet A, Djedjos S, Miller R, Sun X, Hussain MA, Radovick S, Wondisford FE** 2009 Metformin and insulin suppress hepatic gluconeogenesis through phosphorylation of CREB binding protein. Cell 137:635–646
40. **Wang J, Xu J, Finnerty J, Furuta M, Steiner DF, Verchere CB** 2001 The prohormone convertase enzyme 2 (PC2) is essential for processing pro-islet amyloid polypeptide at the NH2-terminal cleavage site. Diabetes 50:534–539
41. **Furuta M, Carroll R, Martin S, Swift HH, Ravazzola M, Orci L, Steiner DF** 1998 Incomplete processing of proinsulin to insulin accompanied by elevation of Des-31,32 proinsulin intermediates in islets of mice lacking active PC2. J Biol Chem 273:3431–3437
42. **Collombat P, Xu X, Ravassard P, Sosa-Pineda B, Dussaud S, Billestrup N, Madsen OD, Serup P, Heimberg H, Mansouri A** 2009 The ectopic expression of Pax4 in the mouse pancreas converts progenitor cells into α and subsequently β cells. Cell 138:449–462